

Radiation-Induced Leukemia at Doses Relevant to Radiation Therapy: Modeling Mechanisms and Estimating Risks

Igor Shuryak, Rainer K. Sachs, Lynn Hlatky, Mark P. Little, Philip Hahnfeldt, David J. Brenner

Background: Because many cancer patients are diagnosed earlier and live longer than in the past, second cancers induced by radiation therapy have become a clinically significant issue. An earlier biologically based model that was designed to estimate risks of high-dose radiation-induced solid cancers included initiation of stem cells to a premalignant state, inactivation of stem cells at high radiation doses, and proliferation of stem cells during cellular repopulation after inactivation. This earlier model predicted the risks of solid tumors induced by radiation therapy but overestimated the corresponding leukemia risks. **Methods:** To extend the model to radiation-induced leukemias, we analyzed—in addition to cellular initiation, inactivation, and proliferation—a repopulation mechanism specific to the hematopoietic system: long-range migration through the blood stream of hematopoietic stem cells (HSCs) from distant locations. Parameters for the model were derived from HSC biologic data in the literature and from leukemia risks among atomic bomb survivors who were subjected to much lower radiation doses. **Results:** Proliferating HSCs that migrate from sites distant from the high-dose region include few preleukemic HSCs, thus decreasing the high-dose leukemia risk. The extended model for leukemia provides risk estimates that are consistent with epidemiologic data for leukemia risk associated with radiation therapy over a wide dose range. For example, when applied to an earlier case-control study of 110 000 women undergoing radiotherapy for uterine cancer, the model predicted an excess relative risk (ERR) of 1.9 for leukemia among women who received a large inhomogeneous fractionated external beam dose to the bone marrow (mean = 14.9 Gy), consistent with

the measured ERR (2.0, 95% confidence interval [CI] = 0.2 to 6.4; from 3.6 cases expected and 11 cases observed). As a corresponding example for brachytherapy, the predicted ERR of 0.80 among women who received an inhomogeneous low-dose-rate dose to the bone marrow (mean = 2.5 Gy) was consistent with the measured ERR (0.62, 95% CI = -0.2 to 1.9). **Conclusions:** An extended, biologically based model for leukemia that includes HSC initiation, inactivation, proliferation, and, uniquely for leukemia, long-range HSC migration predicts, with reasonable accuracy, risks for radiation-induced leukemia associated with exposure to therapeutic doses of radiation. [J Natl Cancer Inst 2006;98:1794-806]

Radiation therapy inevitably exposes normal healthy organs to ionizing radiation and thus involves risks for radiation-induced

Affiliations of authors: Center for Radiological Research, Columbia University Medical Center, New York, NY (IS, DJB); Departments of Mathematics and Physics, University of California, Berkeley, CA (RKS); Department of Medicine, Tufts School of Medicine, Boston, MA (LH, PH); Department of Epidemiology and Public Health, Imperial College Faculty of Medicine, London, U.K. (MPL).

Correspondence to: David J. Brenner, PhD, DSc, Center for Radiological Research, Columbia University Medical Center, 630 West 168th St., New York, NY 10032 (e-mail: djb3@columbia.edu).

See "Notes" following "References."

DOI: 10.1093/jnci/djj497

© 2006 The Author(s).

This is an Open Access article distributed under the terms of the Creative Commons Attribution Non-Commercial License (<http://creativecommons.org/licenses/by-nc/2.0/uk/>), which permits unrestricted non-commercial use, distribution, and reproduction in any medium, provided the original work is properly cited.

Table 1. Properties of different models of radiation-induced cancer for doses relevant to radiation therapy

Initiation*	Processes modeled			Predicted high-dose radiogenic cancer risk	Potential application
	Inactivation†	Proliferation‡	Migration§		
Yes	Yes	No	No	Very small (uncompensated inactivation)	LQE risk estimate
Yes	Yes	Yes	No	Large (proliferation compensates for inactivation)	Solid tumor carcinogenesis
Yes	Yes	Yes	Yes	Intermediate (migration dilutes proliferation)	Leukemogenesis

*Radiation-induced initiation of stem cells (to induce a premalignant state) increases cancer risk.

†Inactivation (i.e., killing) of premalignant cells by radiation decreases cancer risk. Inactivation of normal cells during prolonged irradiation also tends to decrease risk because it depletes the pool of cells that can be damaged by subsequent exposure.

‡Proliferation in response to cellular inactivation takes place during radiation exposure and continues until repopulation is complete. Cellular proliferation expands the numbers of premalignant and normal stem cells, tending to compensate for the effects of cellular inactivation, thereby increasing the cancer risk.

§Long-range migration of mostly normal stem cells from distant, minimally irradiated locations into locations with high radiation-induced damage decreases the cancer risk.

||The excess relative risk estimated by the linear–quadratic–exponential (LQE) model (see equation [1]).

cancer (1–14). Patients treated with radiation therapy for malignancies, such as prostate or breast cancer, are now treated at younger ages and are surviving longer (15,16), resulting in an increased potential for radiation-induced second cancers. The potential for radiation-induced leukemia (6–14) is of particular concern because the period between radiation exposure and the development of leukemia is typically only a few years (9), much less than for the development of most solid tumors (10).

Many epidemiologic studies of cancer risks after radiation therapy have been reported (2–14). However, treatment techniques for radiation therapy are changing rapidly, particularly with increasing use of escalated treatment doses (17–19), altered dose fractionation or protraction (20–23), and altered dose distributions in normal tissues (24,25). Thus, results from these epidemiologic studies, which typically analyze data from treatments that took place several decades ago, cannot be applied directly to modern-day protocols. Evaluating second cancer risks associated with modern-day treatments thus requires the development of mechanistic models that use organ doses or dose distributions as the basis for predicting cancer risks. Such models can also provide insight into the basic biologic mechanisms of radiation carcinogenesis (1).

Radiation therapy can deliver very high doses of radiation to regions in organs that are in or close to the target volume (26). In earlier approaches that estimated the cancer risk associated with high-dose radiation, it was assumed that risk was governed primarily by two competing cellular processes (27)—initiation and inactivation. Initiation is the production of changes that make a cell premalignant, such as chromosomal translocations [e.g., the Philadelphia chromosome (28)], other cytogenetic abnormalities [e.g., point mutations, small-scale chromosomal alterations, chromosomal inversions, deletions, duplications, or aneuploidy (29–31)], or heritable epigenetic alterations. Inactivation is any event that prevents a cell from having any viable progeny (e.g., failing to enter mitosis or undergoing apoptosis).

The assumption that radiation-induced carcinogenesis is primarily governed by initiation and inactivation has generally been quantified by use of the standard linear–quadratic–exponential (LQE) equation [(27); for reviews, see (1,32,33)]. The LQE equation describes the excess relative risk (ERR) of cancer after a single acute dose of radiation (D) as

$$ERR = (aD + bD^2) \exp(-\alpha D - \beta D^2), \quad [1]$$

where a and b are linear and quadratic coefficients for initiation, and α and β are linear and quadratic coefficients for inactivation.

The LQE equation thus uses the classic linear–quadratic form both for radiation-induced initiation ($aD + bD^2$) and for radiation-induced inactivation $\exp(-\alpha D - \beta D^2)$.

For small and intermediate radiation doses, equation [1] predicts that the ERR is an increasing function of dose, as observed in epidemiologic studies (5,6,34,35). At high doses, however, the exponential inactivation term $\exp(-\alpha D - \beta D^2)$ in this LQE equation leads to a very small predicted ERR; i.e., essentially all radiation-initiated premalignant cells would be inactivated by the radiation. As we have shown previously (1), this prediction of the LQE equation is inconsistent with recent risk estimates for radiation-induced solid cancer because such a rapid decrease in the ERR at high doses has not been observed.

Consequently, the standard LQE initiation–inactivation model was extended (1) to include cellular proliferation as a repopulation mechanism for organ stem cells. Symmetric stem cell proliferation (i.e., a stem cell dividing into two daughter stem cells) occurs in response to radiation-induced cellular inactivation (36–39) and replenishes the number of stem cells in an organ. Symmetric proliferation takes place during and after radiation therapy; it tends to counteract the effects of cellular inactivation, thereby increasing ERR (Table 1), because any proliferating stem cell that has premalignant damage can pass that damage on to its progeny. Indeed, in a simplified form of the initiation–inactivation–proliferation model for solid cancer induction, the effects of symmetric proliferation exactly cancel out those of inactivation (1), so that ERR is linear in dose.

In contrast to the LQE initiation–inactivation model, predictions of the newer initiation–inactivation–proliferation model are consistent with current epidemiologic data for radiation therapy–induced solid tumors in organs near the treatment field (1). However, this approach to predicting risks of second cancers is problematic for leukemia, in that measured ERRs for radiation therapy–induced leukemia are lower than those predicted by the initiation–inactivation–proliferation model, although still higher than those predicted by the LQE initiation–inactivation model (5,6,34).

A potential reason for this difference between the risk patterns for high-dose radiation–induced solid tumors and leukemias is the difference in repopulation mechanisms for the relevant target cells. For solid tumors, the target cells are the stem cells for that organ (1); for leukemias, we assume that the cells at risk for radiation-induced initiation to a preleukemic state are hematopoietic stem cells (HSCs), although our results should also apply if, instead, the cells at risk are pluripotent progenitor cells (40). Like other stem cells, HSCs in a given location can repopulate by

symmetric proliferation; unlike other stem cells, they can also repopulate by migrating through the blood stream from distant locations (41–46). Migration of HSCs, occurring primarily through the blood stream, is more rapid and longer ranged than migration of solid organ stem cells (42,43). A substantial fraction of the repopulating HSCs will, therefore, originate far from the radiation treatment volume, in regions in which they were much less likely to have been initiated by radiation to become preleukemic HSCs. In contrast, repopulating stem cells in solid organs will generally have originated in heavily irradiated regions and would, therefore, include an appreciable fraction of premalignant cells. Thus, long-range HSC migration would partially offset the carcinogenic effects of proliferation and would be expected to result in an ERR for leukemia associated with high-dose radiation that is intermediate between the ERR predicted by the initiation–inactivation–proliferation model (which neglects migration) and the ERR predicted by the standard LQE initiation–inactivation model (which neglects both proliferation and migration). In fact, such an intermediate ERR has been observed in epidemiologic studies (5,6,34). In the present study, we extended the initiation–inactivation–proliferation model (1) to apply to leukemias, by adding an analysis of long-range HSC migration to improve the accuracy of risk estimation for leukemias associated with radiation therapy, and to increase mechanistic understanding of radiation leukemogenesis.

SUBJECTS AND METHODS

Radiation-Induced Leukemia Risk Database

The predictions of the model described in this study were validated against the results of a case–control study by Curtis et al. (9) that was based on cancer registry data for women who developed leukemia after radiation therapy for endometrial cancer. The women were treated with a variety of radiation doses, either with fractionated external beam radiation therapy or with a brachytherapy implant that emits radiation at low dose rates.

We chose to analyze the study by Curtis et al. (9) because of the large number (>200) of leukemia patients in that study and because it presented a detailed reconstruction of doses to various parts of the bone marrow. The Curtis study (9) was based on data from nine cancer registries in the United States, Canada, and Denmark, and it analyzed a cohort of 110 000 women with invasive endometrial cancer who were treated with radiation therapy, mostly in the 1960s and 1970s, with a mean treatment year of 1970. That study included 218 women who developed leukemia a mean of 7 years after treatment for endometrial cancer and 775 matched control subjects from the same cohort. Matching was based on registry, age (± 5 years), exact calendar year of treatment, race, survival time, and type of leukemia (acute nonlymphocytic leukemia, acute lymphocytic leukemia, chronic myelogenous leukemia, and chronic lymphocytic leukemia). Four control subjects were chosen for each patient who had a leukemia other than chronic lymphocytic leukemia, and two control subjects were identified for each patient with chronic lymphocytic leukemia. Leukemia risks associated with the radiation doses delivered to the bone marrow were reported (9) for both external beam and brachytherapy treatments. Overall, the radiation exposure approximately doubled the leukemia risk (ERR = 0.9, 95% confidence interval [CI] = 0.3 to 1.9).

Detailed calculations of the distribution of radiation doses across the bone marrow were reported by Curtis et al. (9) for 151

Table 2. Bone marrow mass and dose distributions

<i>j</i>	Bone marrow compartment	% of mass ($100 \times f_j$)*	Normalized compartment-specific marrow dose, cGy/Gy†	
			External beam (a_j)	Brachytherapy (b_j)
1	Cranium	7.6	0.4	0.6
2	Mandible	0.8	0.4	0.6
3	Cervical spine	3.9	0.4	0.6
4	Clavicle	0.8	1.3	1.7
5	Scapula	2.8	1.8	4.0
6	Sternum	3.1	4.4	10
7	Thoracic spine	16.1	8.0	10
8	Ribs (upper)	5.4	2.2	6.3
9	Ribs (middle)	5.4	8.4	10
10	Ribs (lower)	5.4	19	26
11	Lumbar vertebrae (1–2)	4.9	38	33
12	Lumbar vertebrae (3–4)	4.9	79	83
13	Lumbar vertebrae (5)	2.5	335	196
14	Sacrum	9.9	444	288
15	Pelvic bones	17.5	190	288
16	Upper femur	6.7	83	89
17	Humeri	2.3	0.9	2.9

*Percentage distribution (47) of active bone marrow (by mass) in the 17 bone marrow compartments is as indicated. f_j is the fraction by mass in the j th compartment, so that $\sum_j f_j = 1$.

†These values specify how the bone marrow dose is distributed for the brachytherapy or fractionated external beam radiation therapy protocols used in this study (9). The values are bone marrow compartment doses corresponding to a mean (i.e., mass-averaged) bone marrow dose of 100 cGy. Because the compartment doses are normalized to the mean bone marrow dose, $\sum_j f_j a_j = 100$ cGy = $\sum_j f_j b_j$.

patients who developed leukemia and for 564 matched control subjects (Table 2). These 715 subjects constituted two patient populations, one of 188 patients treated with external beam therapy and the other of 527 patients treated with brachytherapy, each of which was divided into four dose groups (D_k , where $k = 1-4$), according to the mean (i.e., bone marrow mass averaged) cumulative dose to the bone marrow. For the population treated with external beam therapy, the values for D_k in the four dose groups, as estimated by Curtis et al. (9), were 6.4 Gy (7 case patients and 28 matched control subjects), 8.8 Gy (19 case patients and 53 control subjects), 10.9 Gy (15 case patients and 36 control subjects), and 14.9 Gy (11 case patients and 21 control subjects), delivered in 20–30 fractions. In our calculations, we assumed that one fraction was delivered every weekday for a 5-week period, for a total of 25 fractions. For the population treated with brachytherapy (average treatment time = 72 hours), values for D_k in the four dose groups were 0.6 Gy (9 case patients and 37 control subjects), 1.2 Gy (12 case patients and 27 control subjects), 1.7 Gy (18 case patients and 49 control subjects), and 2.5 Gy (20 case patients and 75 control subjects).

As discussed above, information about the distribution of dose throughout the bone marrow is important, first because HSCs originating from one part of the bone marrow can migrate to any other part (42) and second because the dose at different locations in the bone marrow can vary by a factor of up to 1000. Curtis et al. used a 17-compartment scheme (9,47), as summarized in Table 2, to describe the dose distribution to different parts of the bone marrow.

The total number of HSCs (N_{tot}) before treatment started was divided into the 17 bone marrow compartments according to the fraction of active bone marrow mass present in each compartment

(9). Thus, if f_j is the fraction of the total bone marrow mass in the j th compartment (Table 2), then the steady-state number N_j of HSCs in that compartment is

$$N_j = N_{\text{tot}} f_j. \quad [2]$$

For the population treated with external beam radiation therapy, the dose d_{kj} per fraction in the j th bone marrow compartment for individuals in the k th dose group is determined by the marrow compartment normalized dose a_j in Table 2 and the mean dose D_k for dose group k as follows:

$$d_{kj} = D_k a_j / F, \quad [3]$$

where the fraction number F is 25.

For the population treated with brachytherapy, the dose rate in the j th bone marrow compartment for individuals in the k th dose group R_{kj} is

$$R_{kj} = D_k b_j / T, \quad [4]$$

where the irradiation time T is 72 hours, and the normalized marrow compartment dose b_j is given in Table 2.

Initiation–Inactivation–Proliferation–Migration Model of Radiation-Induced Leukemia

As discussed above, risks of radiation-induced leukemia at high radiation doses appear to result from a balance between the effects of HSC initiation, inactivation, proliferation, and long-range migration (Table 1). We first consider the general structure of a model that includes these four processes, after which quantification of each of these processes is briefly discussed (for detailed equations, see the Appendix).

The relevant timescale for HSC initiation or inactivation is the actual period of radiation therapy exposure, typically some days or weeks. We assume that proliferation and migration begin soon after treatment starts, continue during treatment, and then typically continue for several months after treatment until HSC repopulation is complete. During this time, the normal HSCs, which are the ones at risk for radiation initiation of preleukemic damage, will vary in number. We write the number at time t after the start of radiotherapy as $n(t)$. The corresponding number of initiated HSCs, $m(t)$, represents preleukemic HSCs capable, with some probability, of eventually causing leukemia. In all realistic scenarios, m is much less than n ; i.e., preleukemic cells constitute only a small fraction of the total HSCs. For example, according to the estimates described below, n is typically a few million, and m is typically a few hundred.

Our model is designed to track the time development of $n(t)$ and $m(t)$ during the period from the start of radiation therapy until HSC repopulation is complete. The quantity of main interest will be m_{radiat} , the number of preleukemic HSCs that are 1) radiation-initiated HSCs or in a lineage originated by a radiation-initiated HSC and 2) viable at the time repopulation goes to completion. As in the initiation–inactivation–proliferation model for solid tumors (1), it will be assumed that ERR is proportional to m_{radiat} , specifically

$$\text{ERR} = B m_{\text{radiat}}. \quad [5]$$

The proportionality factor B depends on the time since repopulation has stopped (essentially the number of years after radiation therapy) and on other demographic and cohort properties (e.g., age at radiotherapy, sex, and ethnicity). However, B does not depend on dose or dose timing as determined by the radiation therapy regimen. Representing ERR as a product of a dose-dependent

term and term depending on cohort properties, as in equation [5], is a standard technique used in modeling radiation-induced carcinogenesis (6,35,48).

After repopulation has run its full course, there are additional, typically much slower, stages in the carcinogenesis process (49–53). The factor B in equation [5] contains the relevant information on these slower processes. Because of its assumed dose independence, B can be estimated from cancer risks derived for atomic bomb survivors who were exposed to lower doses of radiation than the patients treated with radiation therapy. In the next sections, we emphasize estimating the dose-dependent component of the ERR through the quantity m_{radiat} .

Hematopoietic Stem Cell Initiation and Inactivation

Just before irradiation begins, some background preleukemic HSCs may already be present in bone marrow compartments throughout the body or in the blood; we denote their number by m_{init} . We assume in the analysis that m_{init} is much smaller than the total number of HSCs N_{tot} (54,55) and that, just before the irradiation begins, the preleukemic HSCs are uniformly distributed. Thus, from equation [2], the number of preleukemic HSCs in the j th bone marrow compartment is $m_{\text{init}} f_j$.

We describe the net number of viable preleukemic HSCs initiated by a single fraction during multifraction radiation therapy by the standard LQE equation (27), as presented in equation [1], with the parameters a and b proportional to the number of cells at risk for initiation by radiation. Immediately after a dose fraction, d_{kj} is delivered in bone marrow compartment j , the number of viable newly formed preleukemic HSCs is thus

$$n_{kj}(\gamma + \delta d_{kj}) d_{kj} \exp(-\alpha d_{kj}). \quad [6]$$

In equation [6], we have set the quadratic parameter β in the exponential inactivation term equal to zero because survival curves for HSCs are almost purely exponential (56); i.e., $S = e^{-\alpha D}$, where S is the surviving fraction. Parameter estimates involving the initiation constants γ and δ for producing preleukemic cells were derived from atomic bomb survivor data, as detailed below.

For brachytherapy, the dose rates during treatment are sufficiently low that two-track quadratic initiation effects are negligible (57). Thus, the net initiation rate of viable preleukemic HSCs is

$$n_{kj} \gamma R_{kj} - m_{kj} \alpha R_{kj}, \quad [7]$$

where R_{kj} is the dose rate for the j th compartment and the k th dose group. The first term in equation [7], $n_{kj} \gamma R_{kj}$, is a preleukemic HSC initiation rate, and the second term $m_{kj} \alpha R_{kj}$ is the standard cellular inactivation rate for continuous irradiation that corresponds to exponential survival for an acute radiation dose (58,59). As discussed and quantified below, subsequent proliferation of the preleukemic HSCs tends to cancel out the effect of the cellular inactivation term in equation [7] (and in equation [6]), but this cancellation is partially diluted by HSC migration.

Repopulation of Hematopoietic Stem Cells Through Proliferation

Symmetric proliferation of stem cells during and after high-dose radiation increases the risk of radiation-induced cancer [(1) and Table 1]. We assumed that there is a given normal steady-state number N_j of HSCs in each compartment (given by equation [2]) and that, when the total number of HSCs is reduced to less than

this normal steady-state number by radiation inactivation, symmetric HSC proliferation is stimulated. Common mechanisms for increasing the number of HSCs through symmetric proliferation are changes in the fraction of cycling HSCs and/or the length of cell cycle (39). This HSC population expansion can, over a period of days, weeks, or at most several months, gradually restore the steady-state number of HSCs. The expansion rate is quantified by a rate constant, λ , that represents net HSC symmetric proliferation and by a logistic factor that tends to maintain the steady-state number of HSCs in bone marrow. For the k th dose group, the expansion rate of the number of normal HSCs in the j th compartment is then

$$\lambda \{1 - [(m_{kj} + n_{kj})/N_j]\} n_{kj}. \quad [8]$$

For example, if the total number of normal and preleukemic HSCs in the j th compartment is low ($\ll N_j$) because of high-dose radiation inactivation, then the logistic factor $\{1 - [(m_{kj} + n_{kj})/N_j]\}$ in equation [8] is approximately equal to 1, and the number of HSCs increases at a rate that is approximately equal to the maximum rate of λn_{kj} . However, if the HSC number in the j th compartment is high, such as at a distant, minimally irradiated location, then $m_{kj} + n_{kj}$ is approximately equal to N_j , the logistic factor in equation [8] is almost zero, and symmetric proliferation of HSCs in that compartment is essentially zero.

Equation [8] can also be applied to preleukemic HSCs, by exchanging n_{kj} with m_{kj} . Implicit in this procedure is the assumption that normal and preleukemic HSCs have equal per-cell expansion rates, i.e., that the repopulation ratio r , as previously discussed (1), is equal to 1. If appropriate, a growth advantage or disadvantage for preleukemic HSCs during the repopulation period could also be modeled, by allowing the value of the parameter r to be different from 1 (1). Current evidence, however, does not provide a consensus for a growth advantage ($r > 1$) or a growth disadvantage ($r < 1$) for preleukemic HSCs during the repopulation period. The possibility of growth advantages for preleukemic cells during subsequent longer time periods, involving cancer promotion and progression, is implicitly taken into account via the proportionality factor B in equation [5].

We did not include in our model a term for the proliferation of normal and preleukemic HSCs suspended in blood because the contribution from this compartment is likely to be small: HSCs are stimulated to proliferate by the surrounding milieu of other bone marrow cells and the growth factors they secrete, both of which are negligible outside the bone marrow. Even if there was some proliferation in blood, it would have a minimal effect on the numerical results because very few HSCs are in the blood at any one time and because HSCs are in circulation for only a brief period before returning to bone marrow (60). The pool of blood-borne HSCs turns over rapidly (28,29), and so the HSC population in the blood should closely reflect the weighted average concentrations of normal and preleukemic HSCs from all bone marrow compartments.

Repopulation of Hematopoietic Stem Cells Through Migration

Long-range HSC migration from bone marrow to blood, and vice versa, appears likely to strongly influence leukemia risks associated with radiation therapy (Table 1). This migration occurs in response to cytokine signaling (44,45), and it tends to maintain a stable number of HSCs in each bone marrow compartment and in the blood.

We assumed that the rate of immigration of normal HSCs into the j th compartment of the bone marrow from blood for individuals in the k th dose group is given by the expression:

$$C_1 [1 - (n_{kj} + m_{kj})/N_j] v_k f_j, \quad [9]$$

where C_1 is an immigration rate constant, v_k is the number of normal HSCs in blood, f_j is again the fraction of HSCs normally present in the j th marrow compartment, and the term $[1 - (n_{kj} + m_{kj})/N_j]$ is again the logistic factor, as discussed for equation [8]. Equation [9] is also assumed to hold for preleukemic HSCs, with v_k being replaced by μ_k , the number of preleukemic HSCs in the blood.

The rate of the reverse process—emigration of normal HSCs from the bone marrow to the blood—is correspondingly given by

$$C_E [1 - (\mu_k + v_k)/N_{\text{blood}}] n_{kj}, \quad [10]$$

where C_E is the emigration rate constant, n_{kj} is the number of normal HSCs in the j th compartment of the bone marrow, N_{blood} is the steady-state number of HSCs in blood, and $[1 - (\mu_k + v_k)/N_{\text{blood}}]$ is a logistic factor. The same form applies to preleukemic HSCs, if n_{kj} is replaced by m_{kj} . The emigration rate constant C_E can be determined from the immigration rate constant C_1 by the condition that emigration and immigration are equal if all compartments and the blood are depleted of HSCs by a given factor, i.e.,

$$C_E N_{\text{tot}} = C_1 N_{\text{blood}}. \quad [11]$$

Application of the Model to Estimate Radiation-Induced Leukemia Relative Risks

We used the differential and difference equations, equations [A1]–[A13], shown in the Appendix, to implement the HSC initiation–inactivation–proliferation–migration model described above; we then used this implementation to estimate the risk of radiation-induced leukemia for the cohorts of women (9) who were treated by external beam radiation or brachytherapy for endometrial cancer. As discussed below, parameters for the model were derived from biologic measurements of HSCs and were supplemented with two parameters derived from leukemia risk data in atomic bomb survivors who were subject to much lower radiation doses than prescribed in radiation therapy.

Model Parameters

The structure of equation [5] and equations [A1]–[A13] in the Appendix indicates that only the six parameter combinations shown in Table 3 are required to estimate the ERR, under the assumption that the number of preleukemic HSCs is small compared with the number of normal HSCs. We confirmed by direct computation that only these six parameter combinations were needed. As described below, four of these six parameter combinations (α , λ , C_1 , and $N_{\text{blood}}/N_{\text{tot}}$) were directly estimated from biologic data on HSCs, and the remaining two parameters ($\gamma N_{\text{tot}} B$ and $\delta N_{\text{tot}} B$) were estimated from atomic bomb survivor data.

Estimation of Hematopoietic Stem Cell Biologic Parameters

The multiple lineages of blood cells originate in the small population of HSCs that is capable of self-renewal and of generating differentiated progeny (40,61). These HSCs, which we consider to be the most likely target cells for radiation-induced

Table 3. The six essential, independent parameter combinations that are needed to calculate the excess relative risk (ERR) for radiation-induced leukemia

Parameter, units	Interpretation	Default (best estimate)	Reasonable range
1. α , Gy ⁻¹	HSC radiation inactivation parameter*	1.1	0.7–1.5
2. λ , h ⁻¹	HSC number expansion rate constant*	0.001	0.0001–0.004
3. C_1 , h ⁻¹	HSC migration rate constant*†	0.7	0.4–1.0
4. $N_{\text{blood}}/N_{\text{tot}}$	Fraction of HSCs in blood*†	0.0035	0.0017–0.0053
5. $\gamma N_{\text{tot}}B$, Gy ⁻¹ ‡	Leukemia ERR induction: linear parameter§	2.7	0.55–7.1
6. $\delta N_{\text{tot}}B$, Gy ⁻² ‡	Leukemia ERR induction: quadratic parameter§	2.7	0.55–7.1

*Estimated from biologic, rather than epidemiologic, data. HSC = hematopoietic stem cell.

† C_1 and $N_{\text{blood}}/N_{\text{tot}}$ influence the ERR mainly through the product $C_1 \times N_{\text{blood}}/N_{\text{tot}}$.

‡ B is the proportionality constant between ERR and m_{radiat} ; see equation [5].

§The two parameters $\gamma N_{\text{tot}}B$ and $\delta N_{\text{tot}}B$ are appropriately rescaled versions of the constants γ and δ that describe the initiation of normal HSCs by radiation to make preleukemic HSCs. They are estimated from atomic bomb leukemia data, with the risks adjusted to be appropriate for the demographic population under consideration.

||95% confidence interval.

initiation, have been experimentally characterized and mathematically modeled in animals and humans (39,60,62–65). Shochat et al. (63) reported that the total number of HSCs in adult humans N_{tot} was 51000 ± 18000 cells per kilogram of body weight (mean \pm standard deviation [SD]). Udomsakdi et al. (60) reported that the corresponding number of HSCs in adult human blood (called N_{blood} in our model) was 175 ± 30 cells per kilogram of body weight (mean \pm SD). As discussed above, only the ratio $N_{\text{blood}}/N_{\text{tot}}$ of HSCs in blood and bone marrow is relevant for our calculations; from these data, this ratio is 0.0035 ± 0.0018 (mean \pm SD), which is consistent with earlier measurements by Duhrensen et al. (64). A reasonable estimate for the number expansion rate constant λ of these HSCs in adult humans is 0.001 per hour (63), with a biologically plausible range of 0.0001–0.004 per hour (63,65). These values are consistent with the potential doubling times of HSCs measured in mice (39,62). The transition rate constant C_1 of these circulating HSCs, from blood to bone marrow, is less well established in humans, but studies in dogs [for review, see Fliedner (42)] indicate a typical transition rate constant C_1 of 0.7 ± 0.3 per hour (mean \pm SD) (66). Finally, radiation-induced inactivation rates of HSCs can also be estimated from the literature: Typical HSC clonogenic survival curves are exponential in shape; i.e., $S = \exp[-\alpha D]$, where α is the slope and D the radiation dose (56,67). The slope parameter α varies from approximately 0.7 to 1.5 Gy⁻¹, depending on the cell subtype and the extent of cytokine stimulation. In this study, we have assumed that α is the same for normal and preleukemic HSCs.

Estimation of Radiation-Induced Hematopoietic Stem Cell Initiation Parameters

The two additional parameter combinations that are needed to predict leukemia ERRs, $\gamma N_{\text{tot}}B$ and $\delta N_{\text{tot}}B$, involve the constants γ and δ , which characterize radiation-induced initiation of HSCs

(Table 3). These combinations cannot currently be estimated from biologic data because we do not yet know the molecular nature of the key preleukemic lesions and also because the two combinations involve the constant B (see equation [5]), which depends on the details of the cohort under consideration. However, it is possible to appropriately estimate the two relevant parameter combinations $\gamma N_{\text{tot}}B$ and $\delta N_{\text{tot}}B$ from epidemiologic information. In principle, any robust epidemiologic dataset for radiation-induced leukemia could be used, if one assumes that it contains appropriate dosimetry. In practice, as we now discuss, if a dataset involving uniform whole-body irradiation is used, the two parameters $\gamma N_{\text{tot}}B$ and $\delta N_{\text{tot}}B$ can be estimated in a way that is independent of HSC inactivation, migration, and proliferation parameters.

Specifically, when virtually identical doses are delivered to each bone marrow compartment, as for the atomic bomb survivors (35), the model (equations [A1]–[A13]) can be simplified considerably by use of a compensation theorem, illustrated in Fig. 1. In this uniform dosing case, cellular repopulation ultimately compensates exactly for cellular inactivation, so that the overall yield of preleukemic HSCs is equal to the yield of preleukemic HSCs from initiation only, as if cellular inactivation, migration, or proliferation did not occur (i.e., as if $\alpha = 0$, $C_1 = 0$, and $\lambda = 0$). Cellular inactivation, proliferation, and migration individually are by no means negligible in this situation; however, when repopulation is complete, these effects cancel each other out (Fig. 1).

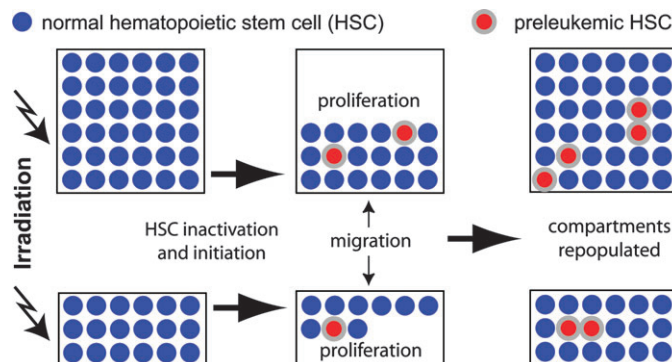


Fig. 1. Compensation theorem. If all bone marrow compartments are exposed to the same radiation dose (as was approximately true for atomic bomb survivors), the initiation–inactivation–proliferation–migration model can be simplified as follows. Hematopoietic stem cell (HSC) proliferation fully compensates for cellular inactivation, and migration is irrelevant because all compartments are exposed to the same dose. Thus, the leukemia risk can be estimated by considering only initiation. This simplification allows the two parameters in the model involving HSC initiation, $\gamma N_{\text{tot}}B$ and $\delta N_{\text{tot}}B$, to be estimated from atomic bomb survivor leukemia data, independent of the other four parameters of the initiation–inactivation–proliferation–migration model. This compensation result is illustrated graphically for a hypothetical, simple case of two bone marrow compartments with different sizes, one containing 36 HSCs and the other containing 18 HSCs. Each compartment receives the same dose of radiation. We assume that this dose causes one of every nine normal HSCs to become preleukemic and inactivates one of every two HSCs. The figure shows how the proliferation and migration of normal and preleukemic HSCs repopulate each compartment. Because the repopulation kinetics are assumed to be the same for normal and preleukemic HSCs, the final results will be that each compartment is filled with HSCs and that one of every nine HSCs is preleukemic, exactly as if inactivation, migration, and proliferation had never occurred, even though all these effects were individually quite large. With the equations in the Appendix, a corresponding result can be proved for an arbitrary number of compartments and/or dose fractions, provided that each marrow compartment receives the same dose of radiation.

For individuals exposed to a uniform single acute dose D , the compensation theorem (Fig. 1), when applied to equation [6], gives the final yield of radiation-initiated HSCs as

$$m_{\text{radiat}} = (\gamma D + \delta D^2) N_{\text{tot}}. \quad [12]$$

Thus, by use of equation [5], the ERR for leukemia induction among individuals exposed to a uniform single acute radiation dose has the following comparatively simple form:

$$\text{ERR} = (\gamma D + \delta D^2) N_{\text{tot}} B. \quad [13]$$

Hence, by fitting equation [13] to the epidemiologic data for leukemia induction in atomic bomb survivors (35), we can estimate the two additional parameters $\gamma N_{\text{tot}} B$ and $\delta N_{\text{tot}} B$ that are needed to predict the leukemia ERR. Such a procedure would, of course, result in parameters that are appropriate to the ethnicity, sex distribution, age at exposure, and time since exposure of atomic bomb survivors. However, as discussed in the context of equation [5], algorithms are available (48,68) to adjust the leukemia ERRs obtained from the atomic bomb survivor cohorts so that they will apply to other cohorts. We used these algorithms to adjust the leukemia ERRs from the atomic bomb survivors to apply to the radiation-therapy cohort in our analysis—specifically, to a Western female population with a mean birth year of 1908, a mean radiation therapy date of 1970, and a mean leukemia diagnosis date of 1977 (9). We used IREP software (version 5.5.1) from the National Institutes of Health (48) for the adjustments. This software is publicly available at www.niosh-irep.com/irep%5fniosh. The algorithm used is essentially the same as that used in the recent National Academy of Sciences BEIR-VII Report (68). Using a modified simulated annealing algorithm (69), we then fit equation [13] to the adjusted dose-dependent ERRs, to obtain parameter estimates for $\gamma N_{\text{tot}} B$ and $\delta N_{\text{tot}} B$; the resulting parameter estimates and 95% confidence intervals are shown in Table 3.

Statistical Analysis

To investigate parameter sensitivity, we calculated the effect of varying, within the biologically reasonable limits shown in Table 3, the values of the four HSC parameters whose estimates were based on biologic considerations (i.e., α , C_1 , λ , and $N_{\text{blood}}/N_{\text{tot}}$). As a further check on the biologic plausibility of the model, we compared the default values of these four HSC parameters (Table 3) that were obtained from the literature and used in our calculations, with the corresponding parameter estimates obtained by directly fitting the model to the radiation therapy data (9). A customized inverse-variance fitting algorithm that was based on simulated annealing (69) was used, with the parameters α , λ , C_1 , and $N_{\text{blood}}/N_{\text{tot}}$ being freely adjustable, apart from non-negativity constraints.

RESULTS

Excess Relative Risk Predictions for Leukemia Induction by Radiation Therapy

Using the default parameter combinations in Table 3, the equations in the Appendix, and equation [5], we obtained ERR predictions, shown in Fig. 2, that are consistent with the data on leukemia induction after brachytherapy or fractionated radiation therapy in the studied population (9). For example, for external

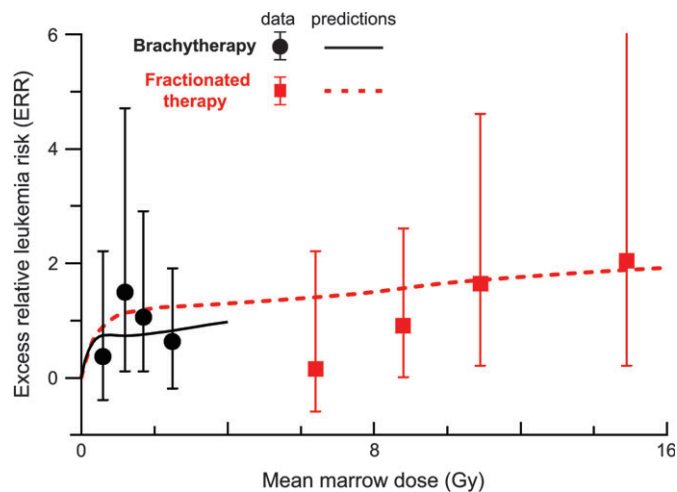
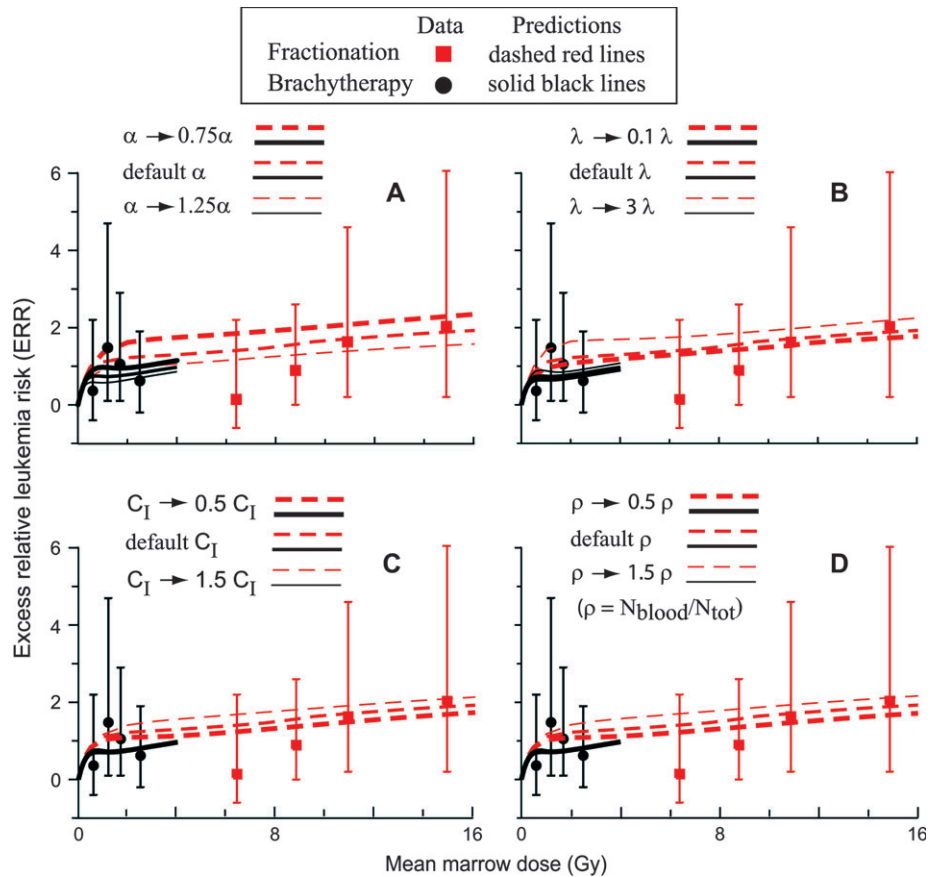


Fig. 2. Model-based predictions for excess relative risk (ERR) of radiation therapy-induced leukemia and corresponding epidemiologic data. **Point estimates** and **error bars** (95% confidence intervals) refer to the data for brachytherapy and fractionated external beam radiation therapy from Curtis et al. (9). The mean total bone marrow dose was averaged by mass over the 17 bone marrow compartments. **Curves** are model predictions (defined by equations [5] and [A1]–[A13]) obtained by use of the default parameter values shown in Table 3. The model predicts a steep initial increase in ERR with increasing dose of radiation, a subsequent leveling off that is much more pronounced than that predicted for solid tumors by the initiation–inactivation–proliferation model without migration, and, in contrast to the standard linear–quadratic–exponential model (equation [1]), predicts a substantial risk even at large doses. The predicted ERRs are consistent with the epidemiologic data.

beam radiotherapy, mean bone marrow doses of 6.4, 8.8, 10.9, and 14.9 Gy were associated with measured leukemia ERRs of 0.14 (95% CI = −0.6 to 2.2), 0.9 (95% CI = 0.0 to 2.6), 1.6 (95% CI = 0.2 to 4.6), and 2.0 (95% CI = 0.2 to 6.4), respectively; the corresponding model-predicted ERRs of 1.4, 1.5, 1.7, and 1.9 were all within the 95% confidence intervals of the data. In the corresponding data for continuous brachytherapy exposure, mean bone marrow doses of 0.6, 1.2, 1.7, and 2.5 Gy were associated with measured leukemia ERRs of 0.35 (95% CI = −0.4 to 2.2), 1.5 (95% CI = 0.1 to 4.7), 1.0 (95% CI = 0.1 to 2.9), and 0.62 (95% CI = −0.2 to 1.9), respectively; the corresponding model-predicted ERRs of 0.71, 0.71, 0.75, and 0.80 were all within the 95% confidence intervals of the data. Because we did not adjust the model parameters to fit the leukemia risks associated with radiation therapy but rather used parameter estimates that were based on biologic data and on atomic bomb survivor data (Table 3) to predict the ERRs associated with radiation therapy, even order-of-magnitude agreement in Fig. 2 was not guaranteed a priori.

As shown in Fig. 2, at low mean radiation doses to the bone marrow (i.e., <1 Gy), the ERR increased approximately linearly with increasing dose. At higher doses (i.e., 1–16 Gy), however, the predicted slope decreased markedly, and thus, the predicted ERR increased only slightly with increasing dose. This decrease in slope can be traced to the predicted effects of long-range HSC migration; it represents a very different prediction both from the standard initiation–inactivation model (27), where the risk is predicted to decrease rapidly at higher doses (i.e., the slope becomes negative), and from the initiation–inactivation–local proliferation model (1), applicable to solid tumors, where the ERR continues to rise substantially throughout this high dose (>1 Gy) range.

Fig. 3. Sensitivity of the predicted leukemia excess relative risk (ERR) induced by radiation therapy to changes in parameters of the initiation–inactivation–proliferation–migration model. In each panel, one hematopoietic stem cell (HSC) biologic parameter was varied within biologically plausible bounds (see Table 3), and the other parameters were fixed at the default values given in Table 3. Results obtained by varying a given parameter are indicated with lines of different thickness. **A)** HSC radiation inactivation parameter α . **B)** HSC number expansion rate constant λ . **C)** HSC migration rate constant C_1 . **D)** Fraction of HSCs in blood $\rho = N_{\text{blood}}/N_{\text{tot}}$. The two remaining relevant parameter combinations, $\gamma N_{\text{tot}} B$ and $\delta N_{\text{tot}} B$, which were determined through atomic bomb survivor data, were kept at the default values shown in Table 3. Because C_1 and ρ influence the ERR primarily through the product ρC_1 , panels C and D are similar to each other. Overall, the model predictions were not substantially sensitive to parameter value variations that were within biologically plausible bounds.



Parameter Sensitivity Studies

We investigated the effects of varying, within biologically plausible limits, the values of the four parameters (i.e., α , C_1 , λ , and $N_{\text{blood}}/N_{\text{tot}}$) whose estimates (see Table 3) were based on biologic considerations. For example, based on the range of parameter estimates in the literature (56,67), the inactivation constant α was varied between 0.75 and 1.25 times the default value (i.e., between 0.83 and 1.4 Gy⁻¹). Varying each parameter within the biologically reasonable ranges shown in Table 3 did not substantially change the predicted dose-dependent ERRs for leukemia induction (Fig. 3).

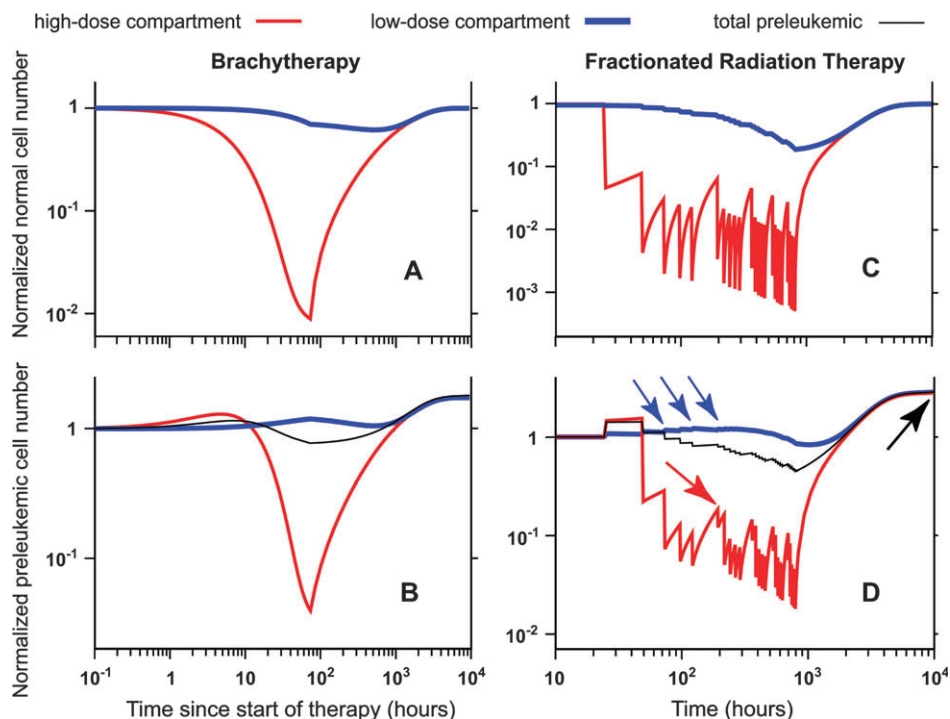
We also fitted the model directly to the radiation therapy data (9) by use of a modified simulated annealing algorithm (69), in which α , λ , C_1 , and $N_{\text{blood}}/N_{\text{tot}}$ were free parameters (i.e., could attain any nonnegative values). We obtained only marginally better fits to the radiation therapy data, compared with the predicted ERRs (Fig. 2) obtained with our default biologically based parameter set (Table 3). When we allowed the parameters to vary to fit the radiation therapy data, we found that, compared with the default values (Table 3), the estimated radiation inactivation parameter α decreased slightly, from 1.1 Gy⁻¹ to 1.0 Gy⁻¹, and that the estimated HSC proliferation rate constant λ also decreased, from 10⁻³ h⁻¹ to 1.2 × 10⁻⁴ h⁻¹. We also found that the estimated migration rate constant C_1 decreased, from 0.7 h⁻¹ to 0.003 h⁻¹, but that C_1 remained much larger than the proliferation rate constant λ . Finally, we found that the estimated parameter $N_{\text{blood}}/N_{\text{tot}}$ increased from 0.3 × 10⁻² to 1.5 × 10⁻². Thus, the HSC parameter values obtained by direct fitting were of the same order as the values estimated (Table 3) from biologic measurements, providing additional evidence that the model is biologically plausible.

Hematopoietic Stem Cell Population Dynamics

The model makes detailed predictions for the dynamics of the HSC populations. Figure 4 illustrates the predicted time courses for the normalized numbers of preleukemic and normal HSCs in a highly irradiated bone marrow compartment, a lightly irradiated bone marrow compartment, and for the entire hematopoietic system. Some general patterns were found that are common to both brachytherapy (Fig. 4, A and B) and fractionated radiation therapy (Fig. 4, C and D). Specifically, in heavily irradiated bone marrow compartments (e.g., the sacrum), the numbers of normal and preleukemic HSCs declined precipitously during the treatment period, by up to four orders of magnitude. After repopulation, however, the final number of preleukemic HSCs in any given compartment was always more than the initial number (e.g., 1.8-fold more for a brachytherapy dose of 2.5 Gy and 2.9-fold more for an external beam dose of 14.9 Gy). In marrow compartments receiving smaller radiation doses (e.g., ribs), cellular inactivation played a smaller role, and the total number of HSCs did not decrease by more than twofold during radiation therapy. As seen in Fig. 4, D, the model predicts that such conditions can produce a small but steady increase in the number of preleukemic HSCs during radiation therapy because the dose delivered by each fraction is sufficiently low that it generates more preleukemic HSCs than it inactivates.

At all times, the predicted fraction of viable preleukemic HSCs in all marrow compartments combined was intermediate between the two extremes of a heavily and a lightly irradiated compartment. For example, as shown in Fig. 4, at the end of radiation therapy but before completion of repopulation, the predicted ratio of the number of preleukemic cells to the number

Fig. 4. Predicted hematopoietic stem cell (HSC) population dynamics during and after radiation therapy. Log-log plots show the evolution over time of normal and preleukemic HSC numbers, normalized to their initial values before treatment. In the examples shown, one bone marrow compartment (i.e., the sacrum, **red line**) received a high radiation dose during therapy and another compartment (i.e., middle ribs, **blue line**) received a much lower dose; the normalized number of preleukemic stem cells summed over all marrow compartments is also shown (**black line**). The curves were calculated by use of the equations of the Appendix, with the default parameter estimates in Table 3. For convenience, the initial number of preleukemic cells was assumed to be $1/B$ (see equation [5]). **A)** Normal cell numbers for continuous brachytherapy (mean bone marrow dose of 2.5 Gy over 72 hours). **B)** Preleukemic cell numbers for continuous brachytherapy (mean bone marrow dose of 2.5 Gy over 72 hours). **C)** Normal cell number for fractionated radiation therapy (mean bone marrow dose of 14.9 Gy delivered in 25 daily acute fractions, excluding weekends, starting after a weekend at $t = 24$ hours). **D)** Preleukemic cell numbers for fractionated radiation therapy (mean bone marrow dose of 14.9 Gy delivered in 25 daily acute fractions, excluding weekends, starting after a weekend at $t = 24$ hours). In the high-dose compartment, strong population fluctuations caused by HSC inactivation and repopulation are evident, especially for weekends. For example, the **red arrow** shows the normalized preleukemic cell number at the start of the second week. In the low-dose compartment, which was located farther away from the treatment field, less inactivation and repopulation are predicted to occur, so that fluctuations are less prominent, and preleukemic HSCs accumulate steadily during the first part of



the regimen (**blue arrows**). The curve for total preleukemic HSCs lies between the curves for the low- and high-dose compartments. The relative increase (**black arrow**) in the number of preleukemic HSCs after a few months, when the normal HSC number has returned to its steady-state value, determines the excess relative risk.

initially present was 0.02, 0.4, or 0.9, respectively, for sacrum, all marrow compartments combined, or ribs. For a given mean dose, the predicted number of preleukemic HSCs after complete repopulation increased by the same factor, compared with the number initially present, in all bone marrow compartments irrespective of the local dose in each compartment. Using the model equations, this result could be traced to intercompartmental migration.

DISCUSSION

Predicting Risks of Radiation Therapy–Related Leukemia

We have shown that a mechanistic initiation–inactivation–proliferation–migration model can provide realistic estimates of dose-dependent leukemia ERRs after radiation therapy by use of 1) biologic data on HSCs and 2) information linking the ERR with the total number of preleukemic HSCs in the body when repopulation is complete. Thus, with this model and appropriate dose distributions in bone marrow (70), it should be possible to predict the, as yet, uncharacterized risks (24) for radiation-induced leukemia associated with more modern radiation therapeutic protocols, such as high-dose intensity-modulated radiation therapy or radiation therapy with altered fractionation or protraction schemes.

Because we currently do not know the exact nature of the key preleukemic lesions, it will be necessary for the foreseeable future to use some epidemiologic data to provide the link between the yield of preleukemic lesions when repopulation is complete and the ERR. In the current work, we used leukemia risks calculated from data on atomic bomb survivors, but the approach

described in the current study could in principle be used to estimate cancer risks in contemporary radiation therapy protocols on the basis of measured risks from earlier radiation therapy treatment protocols.

Such a capability to predict leukemia risks, and the corresponding capability to predict radiation therapy–induced risks for solid cancers (1), gives rise to the possibility of adding second cancer risks to the other quantities (tumor control, early complications, and late-responding complications) that are optimized in state-of-the-art planning for radiation therapy (71).

Dose Dependence of the Leukemia Excess Relative Risk

Each radiation therapy dose fraction (or each period of brachytherapy) produces new preleukemic HSCs and also inactivates a certain percentage of at-risk HSCs and preleukemic HSCs. HSC repopulation is predicted to modulate this picture 1) through migration, mainly of normal HSCs from distant (less irradiated and therefore less damaged) bone marrow sites through the blood to heavily irradiated sites, and 2) through proliferation to increase local numbers of preleukemic and normal HSCs. Analysis of how these different factors interact generated the predicted dose–response curves for leukemia ERR (e.g., Fig. 2).

At low doses (up to ~1 Gy), the predicted leukemia ERRs (Fig. 2) increased approximately linearly with dose. This linearity is the result of a complex interplay that was tracked by the differential and difference equations, as described in the Appendix, for initiation, inactivation, proliferation, and migration. Although the dosimetry is still preliminary (72), epidemiologic data for leukemia mortality after prolonged radiation exposure at the

Techa River in Russia also appear to indicate an approximately linear increase in the ERR up to a dose of 1 Gy (73).

For higher cumulative doses of 1–16 Gy, the slopes of the leukemia ERR curves shown in Fig. 2 decrease markedly as the dose increases, resulting in almost flat dose–response curves. In the current model, this decrease in slope is the result of long-range migration of normal HSCs from minimally irradiated bone marrow compartments to heavily irradiated compartments, an effect that dominates the proliferation of local preleukemic HSCs. For solid cancers, where there is essentially no long-range stem cell migration, such a decrease in slope is much less pronounced, and the ERR continues to rise substantially over this high dose range (1).

Model Limitations

One central aspect of our model is the implicit assumption that the dose–response relation for radiation-induced cancer has the same shape as the dose–response relation for the number of radiation-induced premalignant cells at the time when repopulation is complete. We modeled subsequent longer term evolution of clinical leukemia through a cohort-dependent, but radiation-independent, proportionality factor B in equation [5]. Such an approach is also implicit in most statistically based analyses of radiation-induced cancer (6,35,48) and in many (49,50), but not all (51–53), of the biologically based models of the long-term evolution of premalignant cells.

It is also important to note that the equations used are deterministic in the sense that they deal with numbers of HSCs that are averaged over many patients. If a substantial leukemia risk is associated with even a small number of radiation-initiated preleukemic HSCs, then probabilistic patient-to-patient fluctuations may be important. In such a situation, using probabilistic methods might improve the estimates (74). In fact we have carried out preliminary stochastic modeling (calculations not shown), which indicated that repeated cycles of inactivation and repopulation could produce a highly overdispersed distribution of preleukemic HSCs, which would imply the need to incorporate stochastic corrections into the risk estimates.

Finally, we emphasize the uncertainties of the parameter values of the model, as illustrated in Table 3. There is also some uncertainty associated with the bone marrow distribution data from Cristy (47), as shown in Table 2; for example, there is some indication that adult bone marrow distributions change somewhat with age (75), an effect that could be included as relevant data become available.

Summary

The ability to predict radiation-induced cancer risks associated with modern radiation therapy protocols should allow the risks of second cancers to be included, and potentially minimized, in radiation therapy treatment plan optimization (71). This consideration is of increasing importance in light of the increasing number of younger patients undergoing radiation therapy and with increasing survival times. We have shown that radiation-induced leukemia risks at therapeutic doses of radiation can be predicted with reasonable accuracy with a mechanistically based, but tractable, initiation–inactivation–proliferation–migration model. The model considers initiation (which produces premalignant cells), cellular inactivation, and

cellular proliferation—the key elements in a corresponding model for estimating solid tumor risks. We extended the solid tumor model to leukemia by incorporating an analysis of long-range HSC migration. In addition to providing practical algorithms for the estimation of second cancer risks after radiation therapy, these leukemia and solid cancer models may also provide new quantitative insights into the mechanisms of radiation-induced carcinogenesis.

APPENDIX: MODEL EQUATIONS

In this Appendix, we present the mathematical implementation of the HSC initiation–inactivation–proliferation–migration model for leukemia risk estimation. The implementation is based on differential equations and difference equations, numerical solutions to which were calculated using a customized FORTRAN algorithm.

Brachytherapy

During brachytherapy, radiation is administered at a constant, compartment-specific, low dose rate R_{kj} , as given by equation [4]. In accordance with the biologic concepts discussed in the text, rates of change in the numbers of normal and preleukemic HSCs for the k th dose group and in the j th bone marrow compartment dn_{kj}/dt and dm_{kj}/dt , respectively, are described by the following differential equations:

$$dm_{kj}/dt = [\lambda m_{kj} + f_j C_1 \mu_k][1 - (m_{kj} + n_{kj})/N_j] - C_E m_{kj}[1 - (\mu_k + \nu_k)/N_{\text{blood}}] + [\gamma n_{kj} - \alpha m_{kj}]R_{kj}, \quad [A1]$$

$$dn_{kj}/dt = [\lambda n_{kj} + f_j C_1 \nu_k][1 - (m_{kj} + n_{kj})/N_j] - C_E n_{kj}[1 - (\mu_k + \nu_k)/N_{\text{blood}}] - [\gamma n_{kj} + \alpha m_{kj}]R_{kj}. \quad [A2]$$

In equations [A1] and [A2], the terms involving λ describe an increase in the number of HSCs through symmetric proliferation, the terms involving C_1 describe migration of HSCs from the blood to bone marrow, the terms involving γ describe radiation-induced initiation of normal HSCs to produce preleukemic HSCs, the terms involving α describe radiation-induced inactivation of HSCs, and the terms involving C_E describe migration of HSCs from the bone marrow to blood. For this situation and elsewhere in this analysis, $C_E = C_1 N_{\text{blood}}/N_{\text{tot}}$, from equation [11]. Because m_{kj} is much less than n_{kj} at all times, omitting m_{kj} from the logistic term $[1 - (m_{kj} + n_{kj})/N_j]$ in equations [A1] and/or [A2] has a negligible effect on our final results. Similarly, the number of preleukemic HSCs can be omitted from any or all of the other logistic terms in the equations below without changing our estimates substantially.

Each bone marrow compartment replenishes blood pools with preleukemic and normal HSCs. The rates of change of numbers of preleukemic (μ_k) and normal (ν_k) HSCs in blood are described by the following differential equations:

$$d\mu_k/dt = \sum \{-C_1 \mu_k f_j [1 - (m_{kj} + n_{kj})/N_j] + C_E m_{kj} [1 - (\mu_k + \nu_k)/N_{\text{blood}}]\} + (\gamma \nu_k - \alpha \mu_k)R_k, \quad [A3]$$

$$d\nu_k/dt = \sum \{-C_1 \nu_k f_j [1 - (m_{kj} + n_{kj})/N_j] + C_E n_{kj} [1 - (\mu_k + \nu_k)/N_{\text{blood}}]\} - (\gamma \nu_k + \alpha \nu_k)R_k. \quad [A4]$$

In equations [A3] and [A4], the sums are over the number of bone marrow compartments ($j = 1, \dots, 17$); R_k is the weighted mean radiation dose rate for all bone marrow compartments, representing the radiation dose rate in blood. Because the fraction of HSCs in blood at any one time is small, the final results are highly insensitive to changes in R_k . Equations [A1]–[A4] apply both during the postirradiation part of the HSC repopulation period ($R_{kj} = 0 = R_k$) and during the irradiation period ($R_{kj} > 0$ and $R_k > 0$).

Fractionated and Acute Exposure

For fractionated, external beam radiation therapy, the radiation dose is administered in well-separated dose fractions d_{kj} , given by equation [3]. Between fractions, and after the last fraction, equations [A1]–[A4] hold, with $R_{kj} = 0 = R_k$; however, different equations are needed to describe HSC initiation and inactivation during a treatment fraction.

For computational convenience, the overall radiation therapy treatment period was broken down into discrete time steps (Δt , each of approximately about 0.01 hour). Numerical results were found to be essentially insensitive to step sizes of less than approximately 0.1 hour. We define m_{kj}^- as the number of preleukemic HSCs before a given time step and m_{kj}^+ as the number after the step. The same approach can be used for normal HSCs (n_{kj}^- and n_{kj}^+) and for those suspended in blood (μ_k^- and μ_k^+ for preleukemic HSCs and v_k^- and v_k^+ for normal HSCs). The terms Δm_{kj} , Δn_{kj} , $\Delta \mu_k$, and Δv_k , which represent net rates of proliferation and migration for preleukemic and normal HSC populations per time step, are as follows:

$$\Delta m_{kj} = [\lambda m_{kj}^- + C_1 \mu_k^- f_j][1 - (m_{kj}^- + n_{kj}^-)/N_j] - C_E m_{kj}^- [1 - (\mu_k^- + v_k^-)/N_{\text{blood}}], \quad [A5]$$

$$\Delta n_{kj} = [\lambda n_{kj}^- + C_1 v_k^- f_j][1 - (m_{kj}^- + n_{kj}^-)/N_j] - C_E n_{kj}^- [1 - (\mu_k^- + v_k^-)/N_{\text{blood}}], \quad [A6]$$

$$\Delta \mu_k = \sum \{-C_1 \mu_k^- f_j [1 - (m_{kj}^- + n_{kj}^-)/N_j] + C_E m_{kj}^- [1 - (\mu_k^- + v_k^-)/N_{\text{blood}}]\}, \quad [A7]$$

$$\Delta v_k = \sum \{-C_1 v_k^- f_j [1 - (m_{kj}^- + n_{kj}^-)/N_j] + C_E n_{kj}^- [1 - (\mu_k^- + v_k^-)/N_{\text{blood}}]\}. \quad [A8]$$

In equations [A7] and [A8], the sums are again over the number of bone marrow compartments j ($j = 1, \dots, 17$). By use of equations [A5]–[A8], the updated HSC numbers, after a given time step, have the form:

$$m_{kj}^+ = \{m_{kj}^- + \Delta m_{kj} \Delta t + [\gamma + \delta d_{kj}(t)] d_{kj}(t) n_{kj}^- \} \exp[-\alpha d_{kj}(t)], \quad [A9]$$

$$n_{kj}^+ = \{n_{kj}^- + \Delta n_{kj} \Delta t - [\gamma + \delta d_{kj}(t)] d_{kj}(t) n_{kj}^- \} \exp[-\alpha d_{kj}(t)], \quad [A10]$$

$$\mu_k^+ = \{\mu_k^- + \Delta \mu_k \Delta t + [\gamma + \delta d_k(t)] d_k(t) v_k^- \} \exp[-\alpha d_k(t)], \quad [A11]$$

$$v_k^+ = \{v_k^- + \Delta v_k \Delta t - [\gamma + \delta d_k(t)] d_k(t) v_k^- \} \exp[-\alpha d_k(t)]. \quad [A12]$$

In these equations, $d_k(t)$ is the weighted mean for all bone marrow doses $d_{kj}(t)$, and $d_{kj}(t) = 0 = d_k(t)$, except for those time steps in which a fractionated exposure actually occurs.

In applying the model to atomic bomb data, which we do to estimate the parameters $\gamma N_{\text{tot}B}$ and $\delta N_{\text{tot}B}$, the acute exposures are treated as a special case of the fractionated exposures, with just a single dose fraction and with a uniform dose distribution across the bone marrow.

We developed a customized FORTRAN program to solve equations [A1]–[A12]. The number of radiation-induced preleukemic and normal HSCs were calculated for all times until HSC repopulation is essentially complete.

When HSC repopulation is complete, the numbers of background (m_{init}) and radiation-induced (m_{radiat}) preleukemic HSCs are additive, i.e., the total number of preleukemic HSCs when repopulation has run its course m_{final} is given by

$$m_{\text{final}} = m_{\text{init}} + m_{\text{radiat}}. \quad [A13]$$

The reason for the additivity in equation [A13] is that, before radiation exposure starts, preleukemic HSCs are distributed among the bone marrow compartments in the same proportions as normal HSCs. Let

m' refer only to the initial number of preleukemic HSCs and their progeny—i.e., radiation-initiated preleukemic HSCs and their progeny are excluded—and consider the time course of the ratio of m'/n from the beginning of the irradiation to completion of HSC repopulation. Then, m' and n have essentially the same dynamics with regard to inactivation, proliferation, and migration. In fact, the only difference is the few normal HSCs that are initiated to become preleukemic HSCs by radiation therapy. Because m is much less than n , this difference has a negligible effect on n . This similarity between the dynamics of m' and n implies that m'/n is constant in all compartments at all times, even though m' and n may fluctuate widely. Because eventually n returns to its approximate initial value (apart from a negligible fraction of cells that became preleukemic during irradiation), m' must also eventually return to its initial value. Thus, m_{init} reemerges, essentially unchanged, at the end of the repopulation period and adds to m_{radiat} , as shown in equation [A13].

REFERENCES

- (1) Sachs RK, Brenner DJ. Solid tumor risks after high doses of ionizing radiation. *Proc Natl Acad Sci U S A* 2005;102:13040–5.
- (2) Curtis RE, Freedman DM, Ron E, Ries LAG, Hacker D, Edwards B, et al., editors. *New malignancies among cancer survivors: SEER cancer registries, 1973–2000*. Bethesda (MD): National Institutes of Health; 2006 NIH Publ No. 05-5302. In press.
- (3) van Leeuwen FE, Travis LB. Second cancers. In: Devita VT, Hellman S, Rosenberg SA, editors. *Cancer: principles and practice of oncology*. 7th ed. Philadelphia (PA): Lippincott Williams & Wilkins; 2004.
- (4) Ron E. Cancer risks from medical radiation. *Health Phys* 2003;85:47–59.
- (5) Little MP. Comparison of the risks of cancer incidence and mortality following radiation therapy for benign and malignant disease with the cancer risks observed in the Japanese A-bomb survivors. *Int J Radiat Biol* 2001;77:431–64.
- (6) Travis LB, Andersson M, Gospodarowicz M, van Leeuwen FE, Bergfeldt K, Lynch CF, et al. Treatment-associated leukemia following testicular cancer. *J Natl Cancer Inst* 2000;92:1165–71.
- (7) Brenner DJ, Curtis RE, Hall EJ, Ron E. Second malignancies in prostate carcinoma patients after radiotherapy compared with surgery. *Cancer* 2000;88:398–406.
- (8) Weiss HA, Darby SC, Fearn T, Doll R. Leukemia mortality after X-ray treatment for ankylosing spondylitis. *Radiat Res* 1995;142:1–11.
- (9) Curtis RE, Boice JD Jr, Stovall M, Bernstein L, Holowaty E, Karjalainen S, et al. Relationship of leukemia risk to radiation dose following cancer of the uterine corpus. *J Natl Cancer Inst* 1994;86:1315–24.
- (10) Boice JD Jr, Engholm G, Kleinerman RA, Blettner M, Stovall M, Lisco H, et al. Radiation dose and second cancer risk in patients treated for cancer of the cervix. *Radiat Res* 1988;116:3–55.
- (11) Inskip PD, Kleinerman RA, Stovall M, Cookfair DL, Hadjimichael O, Moloney WC, et al. Leukemia, lymphoma, and multiple myeloma after pelvic radiotherapy for benign disease. *Radiat Res* 1993;135:108–24.
- (12) Boice JD Jr, Blettner M, Kleinerman RA, Stovall M, Moloney WC, Engholm G, et al. Radiation dose and leukemia risk in patients treated for cancer of the cervix. *J Natl Cancer Inst* 1987;79:1295–311.
- (13) Little MP, Weiss HA, Boice JD Jr, Darby SC, Day NE, Muirhead CR. Risks of leukemia in Japanese atomic bomb survivors, in women treated for cervical cancer, and in patients treated for ankylosing spondylitis. *Radiat Res* 1999;152:280–92.
- (14) Thomas DC, Blettner M, Day NE. Case-control study of acute and nonlymphocytic leukemia. *J Natl Cancer Inst* 1992;84:1600–1.
- (15) Farkas A, Schneider D, Perrotti M, Cummings KB, Ward WS. National trends in the epidemiology of prostate cancer, 1973 to 1994: evidence for the effectiveness of prostate-specific antigen screening. *Urology* 1998;52:444–8.
- (16) Brady LW, Kramer S, Levitt SH, Parker RG, Powers WE. Radiation oncology: contributions of the United States in the last years of the 20th century. *Radiology* 2001;219:1–5.
- (17) Zelefsky MJ, Fuks Z, Hunt M, Yamada Y, Marion C, Ling CC, et al. High-dose intensity modulated radiation therapy for prostate cancer: early

- toxicity and biochemical outcome in 772 patients. *Int J Radiat Oncol Biol Phys* 2002;53:1111–6.
- (18) Arriagada R, Komaki R, Cox JD. Radiation dose escalation in non-small cell carcinoma of the lung. *Semin Radiat Oncol* 2004;14:287–91.
- (19) Mangar SA, Huddart RA, Parker CC, Dearnaley DP, Khoo VS, Horwich A. Technological advances in radiotherapy for the treatment of localised prostate cancer. *Eur J Cancer* 2005;41:908–21.
- (20) Stitt JA. High dose rate brachytherapy in the treatment of cervical carcinoma. *Hematol Oncol Clin North Am* 1999;13:585–93, vii–viii.
- (21) Nguyen LN, Ang KK. Radiotherapy for cancer of the head and neck: altered fractionation regimens. *Lancet Oncol* 2002;3:693–701.
- (22) Vicini FA, Vargas C, Edmundson G, Kestin L, Martinez A. The role of high-dose rate brachytherapy in locally advanced prostate cancer. *Semin Radiat Oncol* 2003;13:98–108.
- (23) Pollack A, Hanlon AL, Horwitz EM, Feigenberg SJ, Konski AA, Movsas B, et al. Dosimetry and preliminary acute toxicity in the first 100 men treated for prostate cancer on a randomized hypofractionation dose escalation trial. *Int J Radiat Oncol Biol Phys* 2006;64:518–26.
- (24) Hall EJ, Wu CS. Radiation-induced second cancers: the impact of 3D-CRT and IMRT. *Int J Radiat Oncol Biol Phys* 2003;56:83–8.
- (25) Bucci MK, Bevan A, Roach M 3rd. Advances in radiation therapy: conventional to 3D, to IMRT, to 4D, and beyond. *CA Cancer J Clin* 2005;55:117–34.
- (26) Stovall M, Smith SA, Rosenstein M. Tissue doses from radiotherapy of cancer of the uterine cervix. *Med Phys* 1989;16:726–33.
- (27) Gray LH. A symposium considering radiation effects in the cell and possible implications for cancer therapy. In: *Cellular radiation biology*. Baltimore (MD): William and Wilkins Co; 1965. p. 8–25.
- (28) Radivojevic T, Hoel DG. Modeling the low-LET dose-response of BCR-ABL formation: predicting stem cell numbers from A-bomb data. *Math Biosci* 1999;162:85–101.
- (29) Whang-Peng J, Young RC, Lee EC, Longo DL, Schechter GP, DeVita VT Jr. Cytogenetic studies in patients with secondary leukemia/dysmyelopoietic syndrome after different treatment modalities. *Blood* 1988;71:403–14.
- (30) Christiansen DH, Andersen MK, Desta F, Pedersen-Bjerggaard J. Mutations of genes in the receptor tyrosine kinase (RTK)/RAS-BRAF signal transduction pathway in therapy-related myelodysplasia and acute myeloid leukemia. *Leukemia* 2005;19:2232–40.
- (31) Duesberg P, Rasnick D, Li R, Winters L, Rausch C, Hehlmann R. How aneuploidy may cause cancer and genetic instability. *Anticancer Res* 1999;19:4887–906.
- (32) Bennett J, Little MP, Richardson S. Flexible dose-response models for Japanese atomic bomb survivor data: Bayesian estimation and prediction of cancer risk. *Radiat Environ Biophys* 2004;43:233–45.
- (33) Dasu A, Toma-Dasu I, Olofsson J, Karlsson M. The use of risk estimation models for the induction of secondary cancers following radiotherapy. *Acta Oncol* 2005;44:339–47.
- (34) Little MP. Risks associated with ionizing radiation. *Br Med Bull* 2003;68:259–75.
- (35) Preston DL, Kusumi S, Tomonaga M, Izumi S, Ron E, Kuramoto A, et al. Cancer incidence in atomic bomb survivors. Part III. Leukemia, lymphoma and multiple myeloma, 1950–1987. *Radiat Res* 1994;137: S68–97.
- (36) Sacher GA, Trucco E. Theory of radiation injury and recovery in self-renewing cell populations. *Radiat Res* 1966;29:236–56.
- (37) Brown JM. The effect of acute x-irradiation on the cell proliferation kinetics of induced carcinomas and their normal counterpart. *Radiat Res* 1970;43:627–53.
- (38) von Wangenheim KH, Siegers MP, Feinendegen LE. Repopulation ability and proliferation stimulus in the hematopoietic system of mice following gamma-irradiation. *Exp Hematol* 1980;8:694–701.
- (39) Cheshier SH, Morrison SJ, Liao X, Weissman IL. In vivo proliferation and cell cycle kinetics of long-term self-renewing hematopoietic stem cells. *Proc Natl Acad Sci U S A* 1999;96:3120–5.
- (40) Lessard J, Faubert A, Sauvageau G. Genetic programs regulating HSC specification, maintenance and expansion. *Oncogene* 2004;23:7199–209.
- (41) Hanks GE. In vivo migration of colony-forming units from shielded bone marrow in the irradiated mouse. *Nature* 1964;203:1393–5.
- (42) Fliedner TM. The role of blood stem cells in hematopoietic cell renewal. *Stem Cells* 1998;16:361–74.
- (43) Fliedner TM, Graessle D, Paulsen C, Reimers K. Structure and function of bone marrow hemopoiesis: mechanisms of response to ionizing radiation exposure. *Cancer Biother Radiopharm* 2002;17:405–26.
- (44) Cottler-Fox MH, Lapidot T, Petit I, Kollet O, DiPersio JF, Link D, et al. Stem cell mobilization. *Hematology* 2003:419–37.
- (45) Lapidot T, Dar A, Kollet O. How do stem cells find their way home? *Blood* 2005;106:1901–10.
- (46) Croizat H, Frindel E, Tubiana M. The effect of partial body irradiation on haemopoietic stem cell migration. *Cell Tissue Kinet* 1980;13:319–25.
- (47) Cristy M. Active bone marrow distribution as a function of age in humans. *Phys Med Biol* 1981;26:389–400.
- (48) Land CE, Gilbert E, Smith JM, Hoffman FO, Apostoiaie I, Thomas B, et al. Report of the NCI-CDC Working Group to revise the 1985 NIH radio-epidemiological tables. Bethesda (MD): National Institutes of Health; 2003 DHHS Publ No. 03-5387.
- (49) Armitage P, Doll R. A two-stage theory of carcinogenesis in relation to the age distribution of human cancer. *Br J Cancer* 1957;11:161–9.
- (50) Heidenreich WF, Jacob P, Paretzke HG. Exact solutions of the clonal expansion model and their application to the incidence of solid tumors of atomic bomb survivors. *Radiat Environ Biophys* 1997;36:45–58.
- (51) Bogen KT. Cell proliferation kinetics and multistage cancer risk models. *J Natl Cancer Inst* 1989;81:267–77.
- (52) Luebeck EG, Moolgavkar SH. Stochastic analysis of intermediate lesions in carcinogenesis experiments. *Risk Anal* 1991;11:149–57.
- (53) Sachs RK, Chan M, Hlatky L, Hahnfeldt P. Modeling intercellular interactions during carcinogenesis. *Radiat Res* 2005;164:324–31.
- (54) Bose S, Deininger M, Gora-Tybor J, Goldman JM, Melo JV. The presence of typical and atypical BCR-ABL fusion genes in leukocytes of normal individuals: biologic significance and implications for the assessment of minimal residual disease. *Blood* 1998;92:3362–7.
- (55) Biernaux C, Loos M, Sels A, Huez G, Stryckmans P. Detection of major bcr-abl gene expression at a very low level in blood cells of some healthy individuals. *Blood* 1995;86:3118–22.
- (56) Ziegler BL, Sandor PS, Plappert U, Thoma S, Muller R, Bock T, et al. Short-term effects of early-acting and multilineage hematopoietic growth factors on the repair and proliferation of irradiated pure cord blood (CB) CD34+ hematopoietic progenitor cells. *Int J Radiat Oncol Biol Phys* 1998;40:1193–203.
- (57) Sachs RK, Hahnfeldt P, Brenner DJ. The link between low-LET dose-response relations and the underlying kinetics of damage production/repair/misrepair. *Int J Radiat Biol* 1997;72:351–74.
- (58) Dale RG. The application of the linear-quadratic dose-effect equation to fractionated and protracted radiotherapy. *Br J Radiol* 1985;58:515–28.
- (59) Thames HD. An ‘incomplete-repair’ model for survival after fractionated and continuous irradiations. *Int J Radiat Biol* 1985;47:319–39.
- (60) Udonsakdi C, Lansdorp PM, Hogge DE, Reid DS, Eaves AC, Eaves CJ. Characterization of primitive hematopoietic cells in normal human peripheral blood. *Blood* 1992;80:2513–21.
- (61) Ratajczak MZ, Gewirtz AM. The biology of hematopoietic stem cells. *Semin Oncol* 1995;22:210–7.
- (62) Pietrzyk ME, Priestley GV, Wolf NS. Normal cycling patterns of hematopoietic stem cell subpopulations: an assay using long-term in vivo BrdU infusion. *Blood* 1985;66:1460–2.
- (63) Shochat E, Stemmer SM, Segel L. Human haematopoiesis in steady state and following intense perturbations. *Bull Math Biol* 2002;64:861–86.
- (64) Duhrsen U, Villeval JL, Boyd J, Kannourakis G, Morstyn G, Metcalf D. Effects of recombinant human granulocyte colony-stimulating factor on hematopoietic progenitor cells in cancer patients. *Blood* 1988;72:2074–81.
- (65) Shepherd BE, Guttorp P, Lansdorp PM, Abkowitz JL. Estimating human hematopoietic stem cell kinetics using granulocyte telomere lengths. *Exp Hematol* 2004;32:1040–50.
- (66) Nothdurft W, Steinbach KH, Ross WM, Fliedner TM. Quantitative aspects of granulocytic progenitor cell (CFUc) mobilization from extravascular sites in dogs using dextran sulphate (DS). *Cell Tissue Kinet* 1982;15:331–40.
- (67) Dainiak N. Hematologic consequences of exposure to ionizing radiation. *Exp Hematol* 2002;30:513–28.
- (68) NRC. Health risks from exposure to low levels of ionizing radiation—BEIR VII. Washington (DC): The National Academies Press; 2005.

- (69) Press WH, Flannery BF, Teukolsky SA, Vetterling WT. Numerical recipes: the art of scientific computing. Cambridge (MA): Cambridge University Press; 1986.
- (70) Gershkevitsh E, Clark CH, Staffurth J, Dearnaley DP, Trott KR. Dose to bone marrow using IMRT techniques in prostate cancer patients. *Strahlenther Onkol* 2005;181:172–8.
- (71) Brahme A. Individualizing cancer treatment: biological optimization models in treatment planning and delivery. *Int J Radiat Oncol Biol Phys* 2001;49:327–37.
- (72) Degteva MO, Vorobiova MI, Tolstykh EI, Shagina NB, Shishkina EA, Anspaugh LR, et al. Development of an improved dose reconstruction system for the Techa River population affected by the operation of the Mayak Production Association. *Radiat Res* 2006;166:255–70.
- (73) Krestinina LY, Preston DL, Ostroumova EV, Degteva MO, Ron E, Vyushkova OV, et al. Protracted radiation exposure and cancer mortality in the Techa River Cohort. *Radiat Res* 2005;164:602–11.
- (74) Little MP. A multi-compartment cell repopulation model allowing for inter-compartmental migration following radiation exposure, applied to leukaemia. *J Theor Biol*. In press.
- (75) Ricci C, Cova M, Kang YS, Yang A, Rahmouni A, Scott WW Jr, et al. Normal age-related patterns of cellular and fatty bone marrow distribution in the axial skeleton: MR imaging study. *Radiology* 1990;177:83–8.

NOTES

This work was supported with grants from the National Institutes of Health (U19 AI-67773, P41 EB-002033, P01 CA-49062), the US Department of Energy (DE-FG02-03ER63632, DE-FG02-03ER63668, DE-FG02-01ER63226), NASA (NSCOR NNJ04HJ12, NNJ04HF42G), and the European Commission (FI6R-CT-2003-508842 [RISC-RAD]). The authors had full responsibility for the design of the study, the analysis and interpretation of the (previously published) data, and the decision to submit the manuscript for publication.

Funding to pay the Open Access publication charges for this article was provided by U19 AI067773 from the National Institute of Allergy and Infectious Diseases.

Manuscript received February 15, 2006; revised October 31, 2006; accepted November 2, 2006.